Supplementary Information – Superior thermoelectric properties of ternary chalcogenides $CsAg_5Q_3$ (Q = Te, Se) predicted by first-principles calculations

Un-Gi Jong[a]*, Chung-Jin Kang[a], Su-Yong Kim[a], Hyon-Chol Kim[b], and Chol-Jun Yu[a]†

[a] *Chair of Computational Materials Design (CMD), Faculty of Materials Science, Kim Il Sung University, Pyongyang, PO Box 76, Democratic People's Republic of Korea*

[b] *Institute of Organic Chemistry, Faculty of Chemistry, Kim Il Sung University, Pyongyang, PO Box 76, Democratic People's Republic of Korea.*

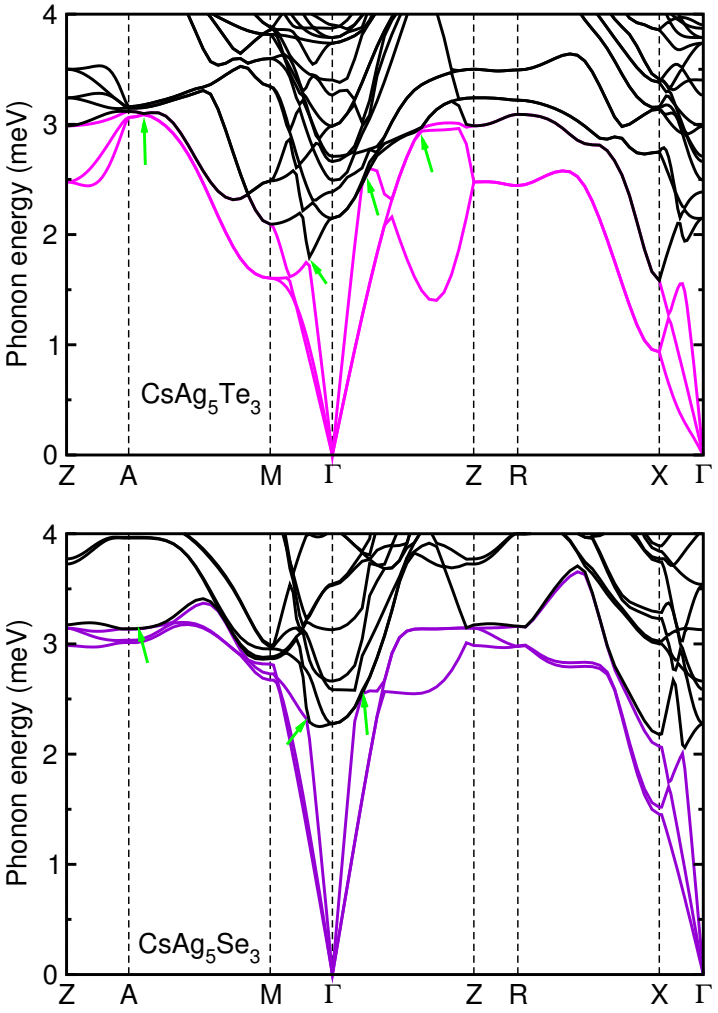

Figure S1. Harmonic phonon dispersion curves within the energy window ranging from 0 to 4 meV for $CsAg_5Q_3$ (Q = Te and Se). The magenta curves represent the three acoustic modes, while the black curves for the optical modes. The green arrows indicate the anti-crossing between the rattling and acoustic modes.

*Un-Gi Jong, Email: ug.jong@ryongnamsan.edu.kp
†Chol-Jun Yu, Email: cj.yu@ryongnamsan.edu.kp

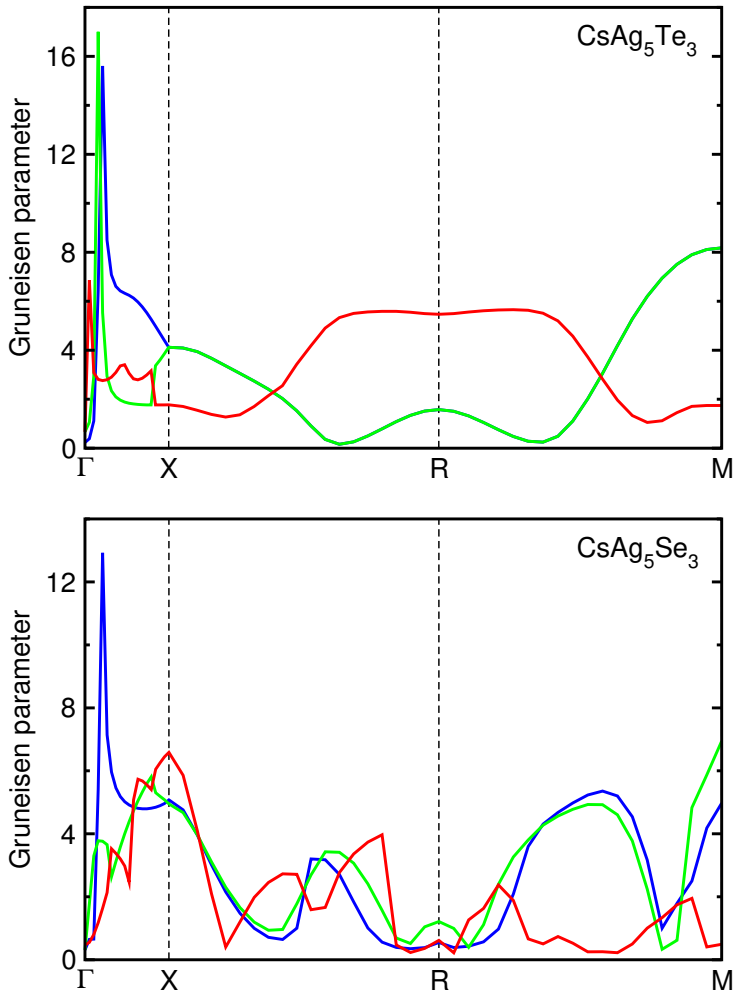

Figure S2. Grüneisen parameters of the acoustic phonon modes along the q-point path Γ–X–R–M of the phonon Brillouin zone for $CsAg_5Q_3$ (Q = Te and Se).

Table S1. Mean square displacements (MSD) of constituent atoms determined by SCP calculations at 300 K in $CsAg_5Q_3$.

	MSD (Å^2)	
Atom	Q = Te	Q = Se
Cs	0.0200	0.0200
Te1	0.0134	0.0129
Te2	0.0136	0.0130
Ag1	0.0226	0.0219
Ag2	0.0170	0.0159
Ag3	0.0262	0.0241

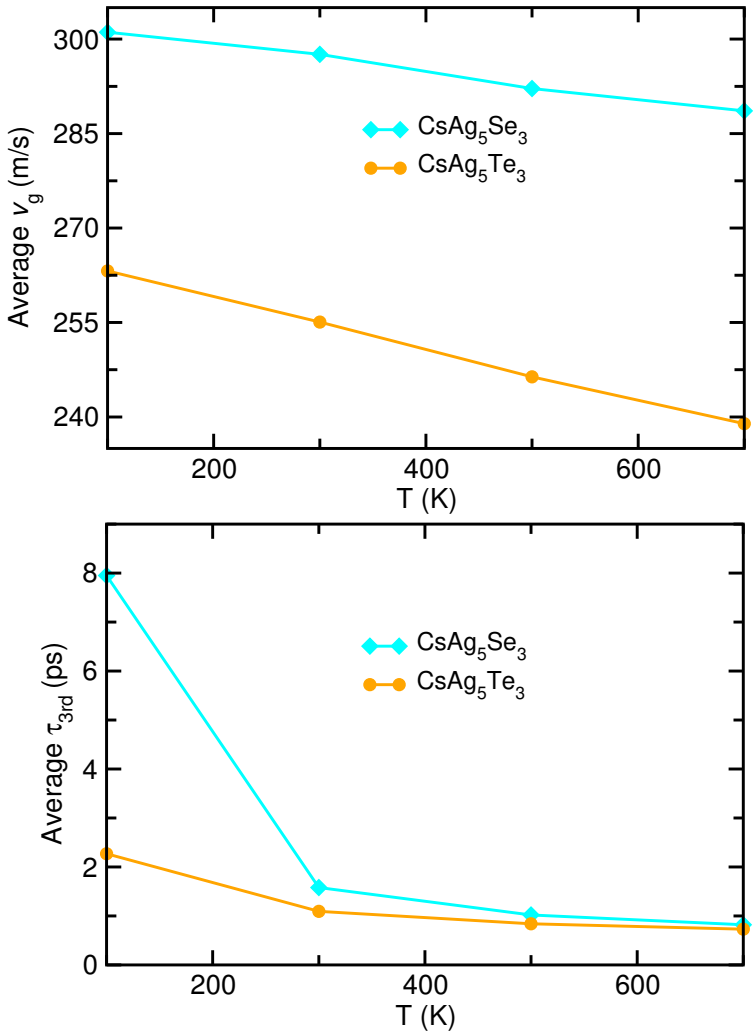

Figure S3. Average phonon group velocity v_g and phonon lifetime τ_{3rd} estimated from the SCP calculations at temperatures ranging from 100 to 700 K with a step of 100 K for $CsAg_5Q_3$ (Q = Te and Se).

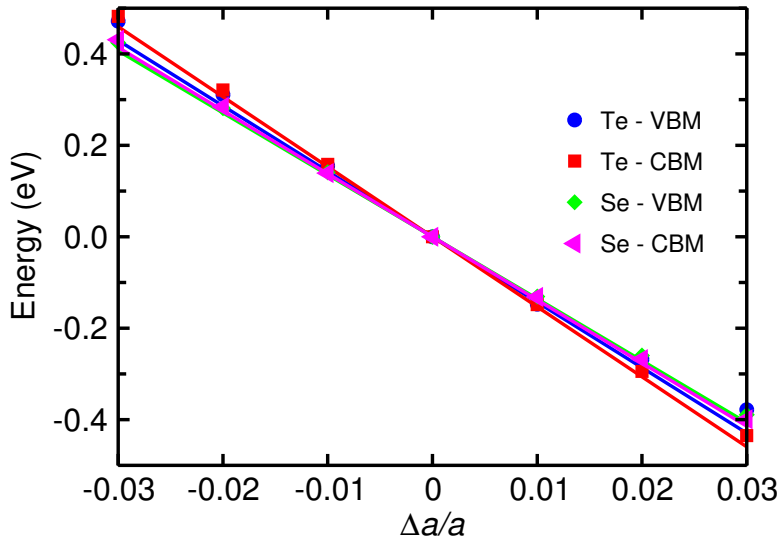

Figure S4. Deformation potential D calculated with mBJ functional for $CsAg_5Q_3$ (Q = Te and Se).

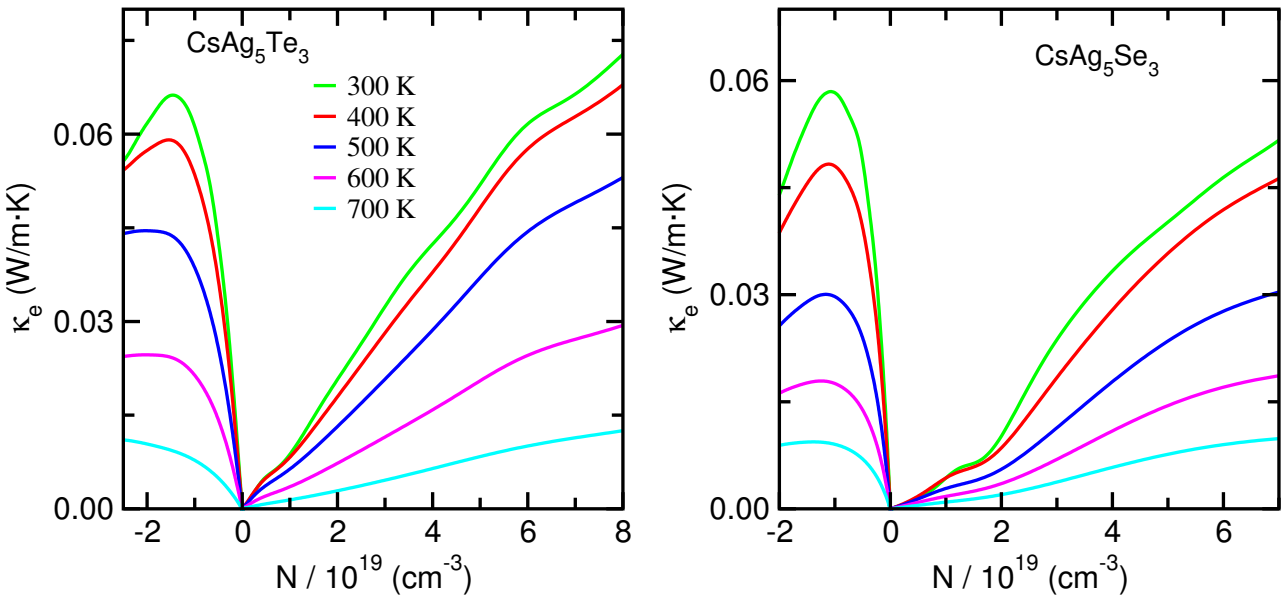

Figure S5. Average electron thermal conductivity κ_e as a function of carrier concentration at different temperatures for $CsAg_5Q_3$ (Q = Te and Se).

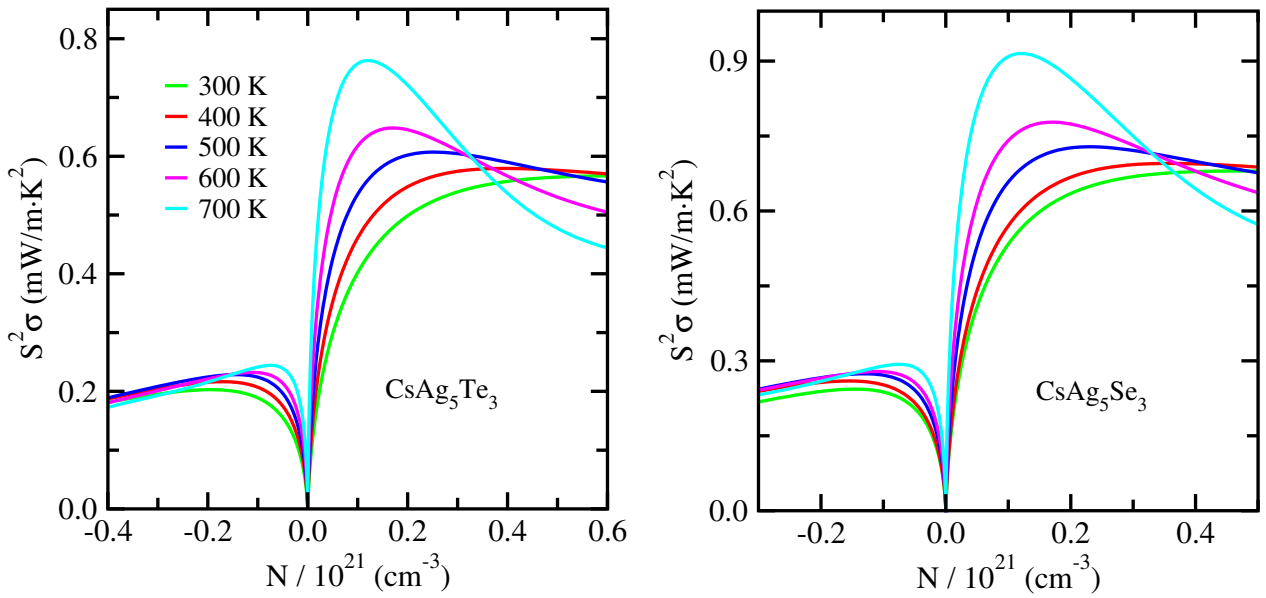

Figure S6. Average thermopower factor $S^2\sigma$ as a function of carrier concentration at different temperatures for $CsAg_5Q_3$ (Q = Te and Se).

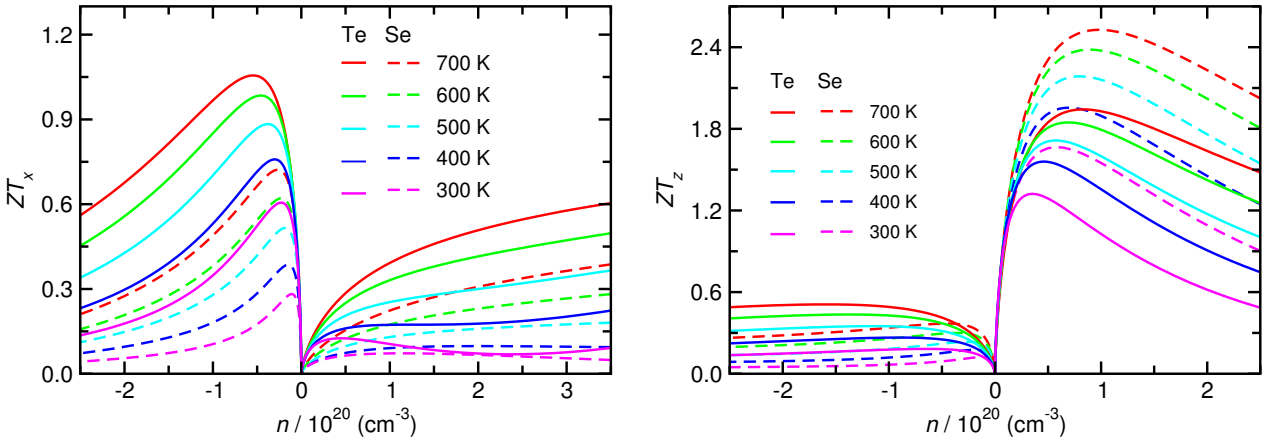

Figure S7. Thermoelectric figure of merit ZT_x (= ZT_y) and ZT_z along x- and z-axises as a function of carrier concentration at different temperatures for $CsAg_5Q_3$ (Q = Te and Se).

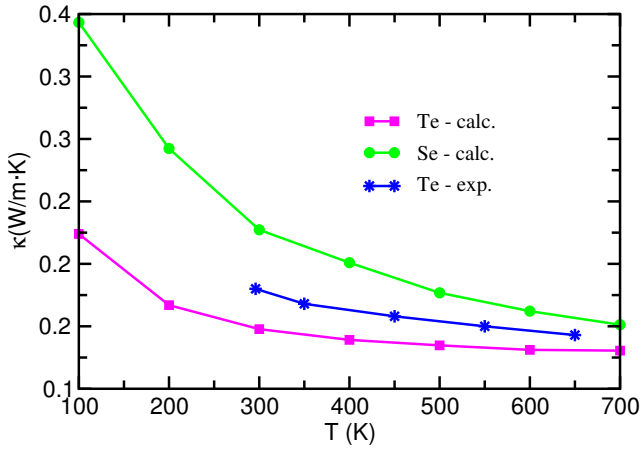

Figure S8. Average lattice thermal conductivity κ_l at different temperatures for $CsAg_5Q_3$ (Q = Te and Se).

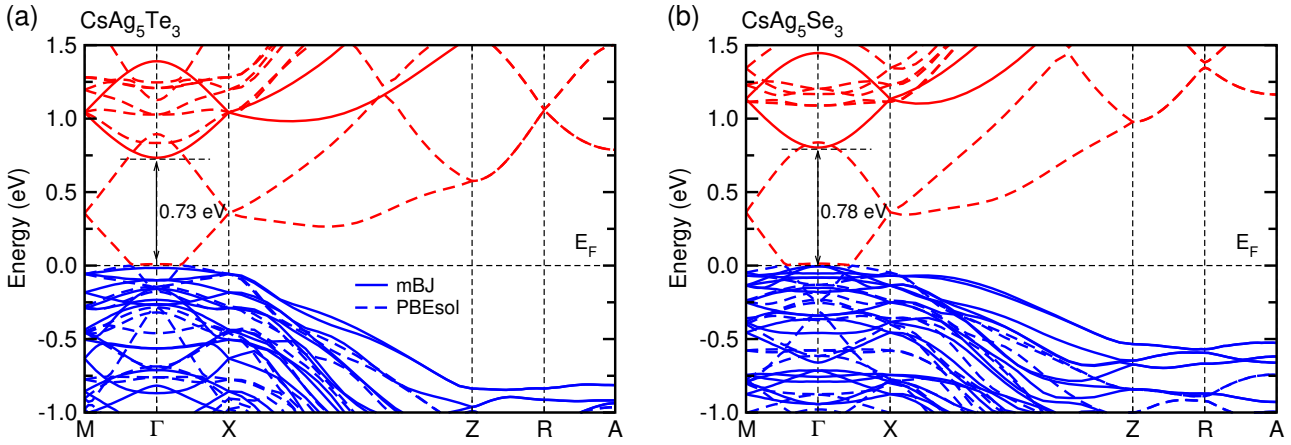

Figure S9. Electronic band structures for (a) $CsAg_5Te_3$ and (b) $CsAg_5Se_3$, calculated by using PBEsol (dashed lines) and mBJ (solid lines) functionals. Valence (conduction) bands are denoted by blue (red) colour, and the valence band maximum is set to zero.

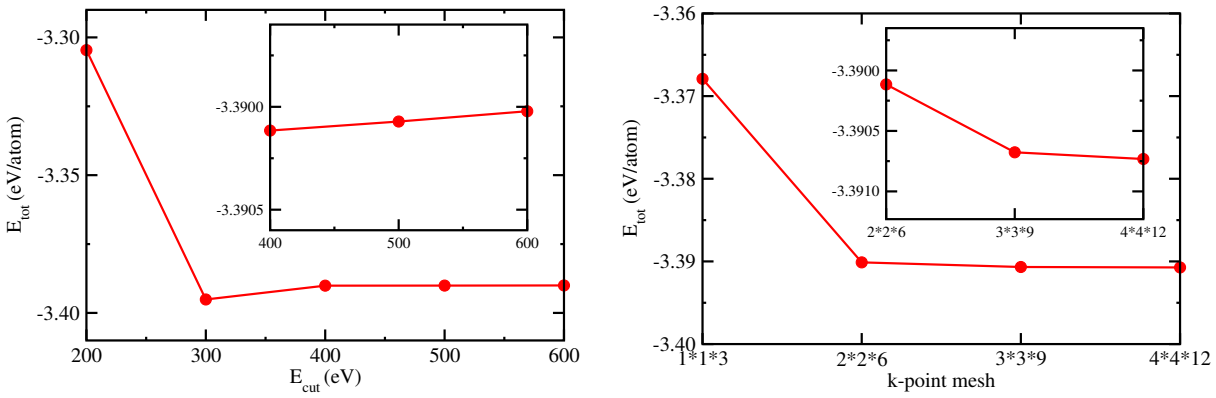

Figure S10. Total energy (E_{tot}) as increasing the cut-off energy (E_{cut}) with fixed k-point mesh of $(2 \times 2 \times 6)$ and as increasing the k-point mesh with fixed cut-off energy of 600 eV for $CsAg_5Te_3$.